Key Engineering Materials
ISSN: 1662-9795, Vol. 804, pp 23-27
doi:10.4028/www.scientific.net/KEM.804.23

Submitted: 2018-08-30
Revised: 2018-11-07
Accepted: 2018-12-06
Online: 2019-05-29

Study on Development of Novel Mg-Based Alloys by Rapid Solidification Technology of Twin Roll Casting

Haijian Wang[1,a], Zhipu Pei[1,b] and Dongying Ju[2,c*]

[1]Department of Material Science and Engineering, Saitama Institute of Technology Fusaiji1690, Fukaya, Saitama 369-0293, Japan

[2]Department of Material Science and Engineering, University of Science and Technology Liaoning, No.185 Qianshan Mid-Road, Anshan, Liaoning,114051,China

[a]e7002qox@sit.ac.jp, [b]peizhipu@gmail.com, [c]dyju@sit.ac.jp

Keywords: Metallic glasses; rapid solidification; quasi-amorphous; GFA.

Abstract. Mg-based alloys were prepared by rapid solidification of twin roll casting (TRC). Then microstructure and element distribution were investigated by means of scanning electron microscope (SEM) and electron probe micro analyzer (EPMA). The analyze microstructure and crystal structure of Mg-based alloys were characterized by X-ray diffraction and transmission electron microscope (TEM). The designed Mg-rare-earth (RE) alloy with quasi-amorphous and fine crystalline dual -phase microstructure was produced by rapid solidification using TRC process. The rapid solidification process was realized by a faster casting speed and a thinner roll gap without anther additional devices and vacuum environment. EPMA results and TEM analyses show that the quasi-amorphous phase had a high concentration in Al and RE element. A quasi-amorphous phase surrounded by dendrites phase and normal crystals in the middle of Mg-Re alloy was observed .

1. Introduction

Metallic glasses are currently the focus of intense research in the international metals community due to their special microstructure and properties [1]. However, it is still a mystery about those questions on the development, structure and physical properties of this new phase. Glass-forming systems have been found in all major bonding classes, including covalent, ionic, van der Waals, hydrogen bond, and metallic [2]. The forming of metallic glasses (MGs) needs extremely high cooling rates (on the order of 10^5 to 10^6 K/s) due to the non-directional nature of metallic bonds and the fact that metals are comprised of individual spherical atoms, as opposed to non-spherical compounds such as SiO_2 and other oxide glasses. In the case of, since individual atoms can rearrange quickly into lower energy configurations or crystalline phases, a higher cooling rate is required to avoid crystallization [3].

In 1970, Twin roll casting (TRC) technique for preparing uniform films of metastable phases was developed by Chen and Miller [4]. To date, this technique in producing metallic glass ribbons is almost limited to laboratory scale studies; however TRC is an available process for producing amorphous alloy sheets with a wide range of cooling rates. In this work, we focused on developing a new kind of Mg-based alloy with the quasi-amorphous phase. Considering its application, we proposed a cost-competitive method to produce the new material in sheet form. It considered as an efficient mass-production technique.

2. Alloy Composition Design

The glass forming ability rules in Mg-based materials. Mismatch entropy normalized by Boltzmann constant (S_{ζ} / k_B) based on hard sphere model and mixing enthalpy (ΔH) based on regular solution model were expressed as a function of composition in multicomponent systems by Takeuchi [5] and Inoue [6]. Atomic size distribution plots for the glass forming ability (GFA) were proposed by Senkov [7]. It was found that a concave upward distribution correlates so strongly with improved glass forming ability. Mg-based alloys are deviate from this trend. This is another exception of Mg-based materials.

Compositions of the alloys. In order to retain an expect structure from the melt, (1) appropriate quenching techniques must be applied, and (2) careful alloy selection must be made. Considering from the topological aspect, atomic radii of candidate alloying elements for magnesium alloys are listed in Table 1. Atomic size differences between the alloying elements and magnesium (aluminum) are also calculated which symbolized by ASD_{Mg} (ASD_{Al}).

Table 1. Atomic radius of some common elements used in Mg alloys.

Elements	Mg	Al	Si	Mn	Zn	In	Sn	Ce	La
Radius / nm	0.160	0.143	0.134	0.132	0.139	0.166	0.158	0.182	0.187
ASD_{Mg} / %		10.625	16.25	17.5	13.125	3.75	1.25	13.75	16.875
ASD_{Al} / %	11.888		6.294	7.692	2.797	16.084	10.490	27.273	30.7[illegible]

Table 2. Composition of the AZ31-In-Sn alloy

Elements	Mg	Al	Zn	In	[illegible]
at%	94.378	5.188	0.247	0.1[illegible]7	0.06[illegible]
wt%	92.768	5.655	0.697	0.5[illegible]	0.[illegible]9

Table 3. Composition of the Mg-RE alloy

Elements	Mg	Al	Si	Mn	Zn	La	Ce
at%	94.6	3.99	0.107	0.12[illegible]	0.04358	0.464	0.66
wt%	89.2427	4.1779	0.1169	0.[illegible]550	0.1106	2.5007	3.5963

AZ31B is a popular wrought magnesium alloy used in many aerospace and automotive applications. However, its widespread apply is hindered by the poor corrosion resistance and low ductility. As Sn has the potential of improve corrosion resistance and ductility of Mg-Al alloy [8], In is used in Mg battery materials [9]. With the purpose of trying to find out whether it can form an amorphous phase contained material through the rapid solidification of TRC method in the current study, AZ31-In-Sn alloy was studied in this work. AZ31 alloy was adopted as a material for contrast.

Rare earth (RE) element has a characteristic of so-called–scavenger effect in magnesium alloys [10]. Impurity elements could form less cathodic intermetallic compounds with RE. In order to improve the corrosion resistance of the product, lanthanum and cerium were adopted in our designment. The composition after melted by high frequency induction melting are listed in Table 2 and Table 3 and the real compositions were tested by X-ray fluorescence (XRF) analysis method.

3. Experiments and Discussion

Microstructure characteristic. In order to achieve a faster cooling rate by the TRC process, we set the speed of the rolls at [illegible]0rpm, Considering the separating force generated during casting, a metal block was set at the moving roll side to form a supporting force, to make a narrow roll gap during casting process as much as possible.

The SEM image of the AZ31 alloy strip with thickness of 1.2 mm is shown in Fig. 1(a). It has an average secondary dendrite arm spacing (DAS) of about 0.7 μm. It is found that the Mg is uniformly distributed in this area due to the very fine dendrite. It is quite difficult to obtain a glassy state of AZ31 alloy even though we set a faster cooling rate hardly. Fig. 1(b) shows the cross-sectional SEM image obtained near the sliced surface. There are a number of fine grains having sizes of 0.5~2 μm due to the effect of chilling. Although a narrow DAS at the center of the slice and fine grains near the surface of the slice formed during the rapid cooling process, a crystalline phase is observed under such a limit condition of the twin roll caster. SEM images of Mg-RE alloy sheet are shown in Fig. 1(c). The microstructure mainly characterized by fine equiaxed grains and dendrites with closely spaced secondary dendrite arms. Meanwhile, there are some special areas having no appreciable crystalline features indicated by the red arrows. We name them quasi-amorphous solids, and the structure was characterized by the following X-ray diffraction (XRD) and transmission electron microscopy (TEM) analysis. Critical cooling rate for forming metallic glass with the composition of the quasi-amorphous phase regions is lower than that of the crystalline phase regions, in other words, the glass forming ability (GFA) of the Mg-RE is higher.

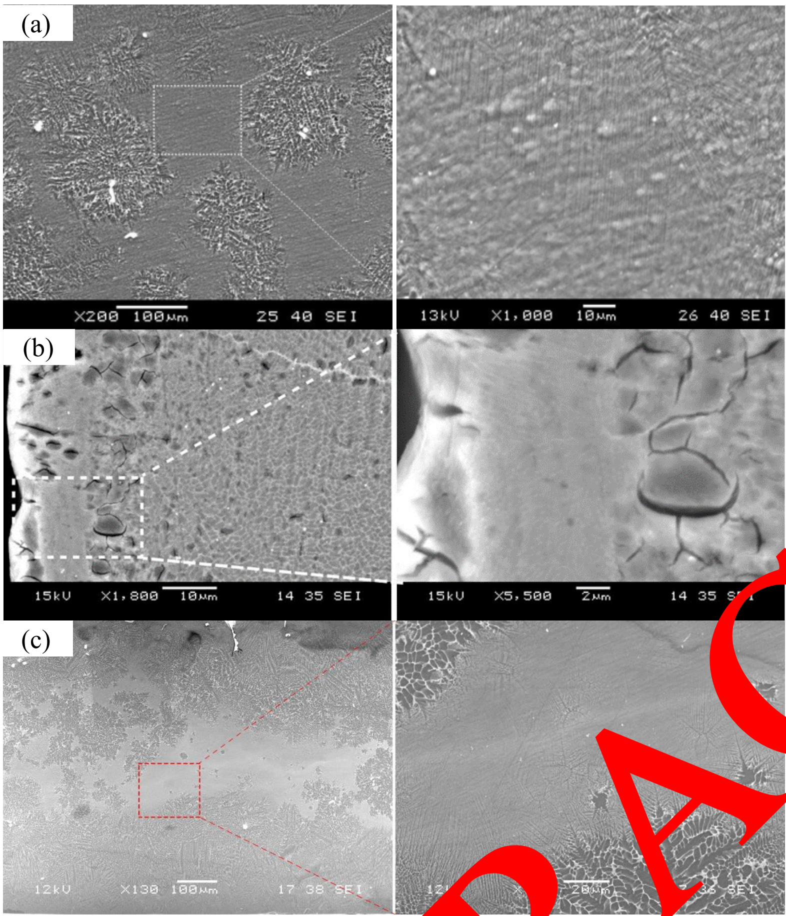

Fig.1. SEM image of as-cast (a) AZ31 alloy, (b) AZ31-In-Sn alloy, (c) Mg-Re alloy sheet in transverse section.

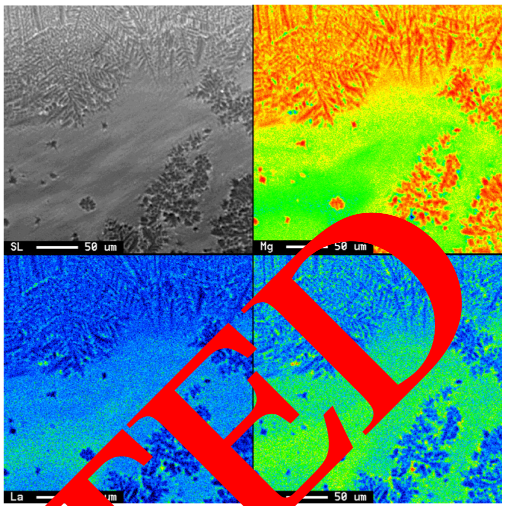

Fig.2. EPMA mapping of the Mg-Re alloy sheet—large quasi-amorphous phase.

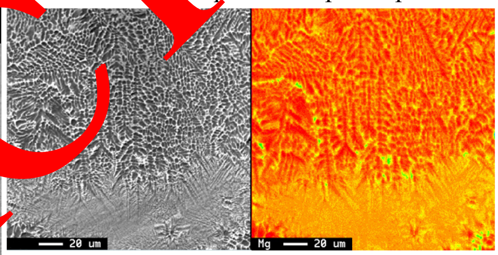

Fig.3. EPMA mapping of the Mg-RE alloy sheet—small quasi-amorphous phase

Elements distribution maps of the Mg-RE alloy sheet sample were obtained by electron probe micro-analysis (EPMA), as shown in Fig. 2 and 3. On the one hand, element segregation exists between the crystalline phase matrix and the quasi-amorphous phases. On the other hand, it is shown that grain boundary segregation forms easily as the atomic size difference (ASD) between Mg and alloying element is larger than 10%. As the atomic sizes between Mg-Al, Mg-La, Mg-Ce, Al-La and Al-Ce are quite different, dendritic segregations also generate in the crystalline matrix.

Based on the EPMA analyses of Fig. 2 and 3, microstructure characteristic of the quasi-amorphous phase and its surroundings are illustrated in Fig. 4. At zone A shows the crystalline matrix with fine equiaxed grains and dendrites, segregation of elements occurs at the grain boundaries and dendrite spaces. At zone B where fine dendrites with closely spaced secondary dendrite arms distributed around a large quasi-amorphous phase, element segregation of this zone decreased due to the fine dendrites. Elements uniformly distribute the quasi-amorphous phase as indicated by zone C. It contains a low amount of Mg comparing to the crystalline matrix. Contrarily, the amount of Al and La is relatively large. Although a few nuclei inside the quasi-amorphous phase, their growths are restricted and the final sizes are less than 20 µm.

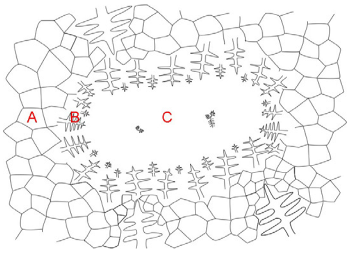

Fig.4. Schematic illustration of microstructure characteristic of the quasi-amorphous phase and its surroundings.

X-ray diffraction analysis

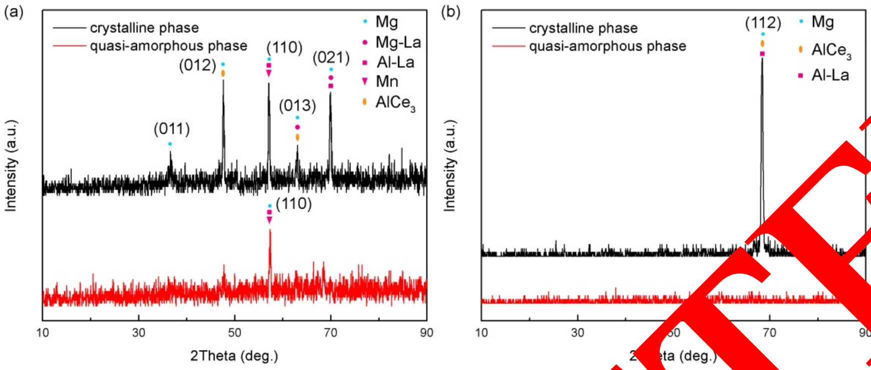

Fig.5. μ-XRD patterns of the as-cast sheet mid-thickness: (a) small quasi-amorphous phase with crystalline structure; (b) large quasi-amorphous phase without crystalline structure.

Micro-XRD (μ-XRD) patterns obtained from the as-cast Mg-RE alloy sheet sample are shown in Fig. 5 Several diffraction peaks appear in the profile obtained from the crystalline phase. A weak peak in the quasi-amorphous phase at 2θ=57.4°, because the area of tested region was smaller than collimated incident beam (Φ=0.03 mm) and some of the crystalline phase information was mixed in it. Another reason of the peak is the find dendrites existed in the large quasi-amorphous solids, as shown in Fig. 1(c). In Fig. 5(b), the μ-XRD pattern obtained from the crystalline phase exhibits only one peak at 2θ=68.4°. This may due to the detection area contains a single crystal and a small quasi-amorphous phase.

TEM analysis. TEM images of the as-cast Mg-RE alloy shown in Fig. 6. SAED patterns are also shown in the insets. In Fig. 6(a) the grain consists of Mg crystal having a grain size of 5 μm. According to model we proposed in Fig. 4, the Mg crystal corresponds to the zone A. The very fine grains with average grain size of 0.[illegible] μm are observed in Fig. 6(a) and (b). These area corresponding to the zone B in Fig. 4. The SAED pattern reveal that these grains are Mg-La phase.

TEM image of [illegible] grain and its grain boundary and the corresponding SAED patterns are shown in Fig. 6(d). The Mg grain size is 7 μm. Near the grain boundary, there also an amount of very fine grains with size of 0.[illegible] μm. These grains are identified as Mg-La and Al-La phases. It indicates that these two phases precipitated at the Mg grain boundaries during the rapid speed solidification. The border of the zone B and C in Fig. 4 correspond to Figs. 6(e) and (f). In the zone B, it contains fine dendrites feature. In the zone C, it shows a poor crystallinity. Some diffraction spots appears in the SAED patterns, because the size quasi-amorphous phase was small or the specimen damaged due to the electron irradiation.

4. Conclusion

The designed Mg-RE magnesium alloy with quasi-amorphous phase and fine crystalline phase dual phase microstructure produced with the rapid solidification of TRC process. The rapid solidification process realized by a faster casting speed and a thinner roll gap without additional devices and vacuum environment. EPMA results and TEM analyses show that the quasi-amorphous phase has a high concentration in Al and RE element, which results in the fact that the Mg-RE alloy had a better GFA.

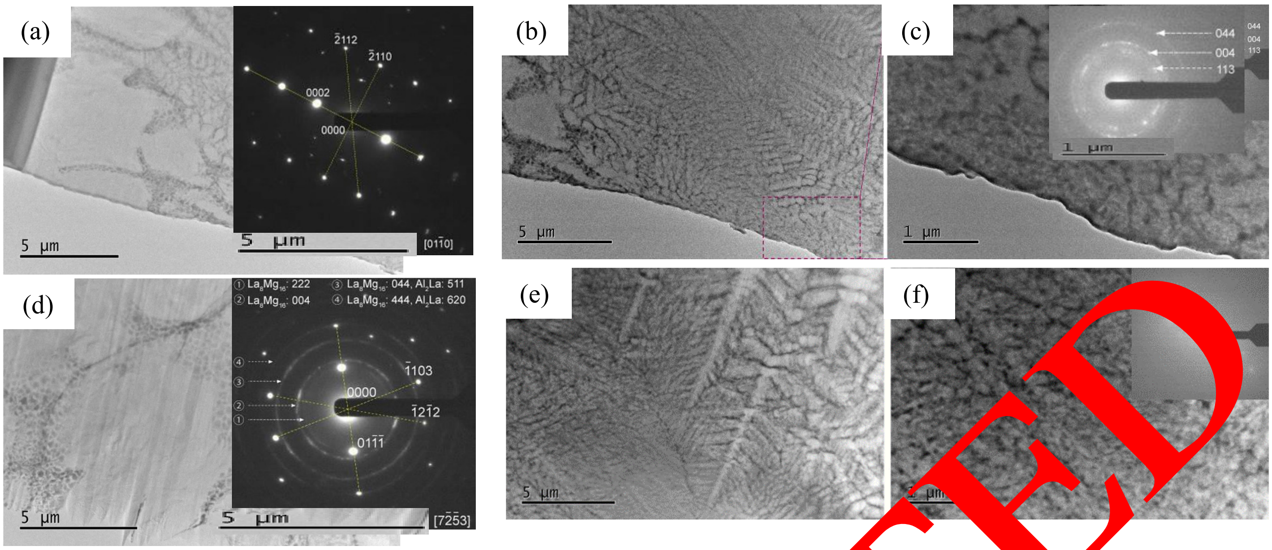

Fig.6. TEM image of the as-cast Mg-RE alloy. Inset, SAED pattern of Mg grain — (a) Mg-RE alloy; (b) (c) La_8Mg_{16} phase; (d) Mg grain and La-Mg, Al-La phase at grain boundary; (e) fine dendrites; (f) quasi-amorphous phase.

Acknowledgement

This work was supported by Cooperative Research and Development Center for Advanced Materials (CRDAM) funded by the Institute for Materials Research (IMR), Tohoku University (Project Number 18G0042).

References

[1] Green A L, Ma E. Bulk Metallic Glasses: At the Cutting Edge of Metals Research [J]. MRS Bulletin, 2007, 32(08): 611-619.

[2] Susanne S. Bulk metallic glasses [J]. Journal of Physics: Condensed Matter, 2001, 13(34): 7723.

[3] Arata E R. High temperature ultrahigh-gravity centrifugal processing of metallic melts [D]; Citeseer, 2008.

[4] Chen H S, Miller C E. A Rapid Quenching Technique for the Preparation of Thin Uniform Films of Amorphous Solids [J]. Review of Scientific Instruments, 1970, 41(8): 1237-1238.

[5] Takeuchi A, Inoue A. Calculations of Mixing Enthalpy and Mismatch Entropy for Ternary Amorphous Alloys [J]. Materials Transactions, JIM, 2000, 41(11): 1372-1378.

[6] Inoue A. Bulk amorphous and nanocrystalline alloys with high functional properties [J]. Materials Science and Engineering: A, 2001, 304-306(1): 1-10.

[7] Senkov O N, Miracle D B. Effect of the atomic size distribution on glass forming ability of amorphous metallic alloys [J]. Materials Research Bulletin, 2001, 36(12): 2183-2198.

[8] She J, Pan F, Zhang J, et al. Microstructure and mechanical properties of Mg–Al–Sn extruded alloys [J]. Journal of Alloys and Compounds, 2016, 657(1): 893-905.

[9] Murgia F, Weldekidan E T, Stievano L, et al. First investigation of indium- based electrode in Mg battery [J]. Electrochemistry Communications, 2015, 60(1): 56-59.

[10] Liu W, Cao F, Chang L, et al. Effect of rare earth element Ce and La on corrosion behavior of AM60 magnesium alloy [J]. Corrosion Science, 2009, 51(6): 1334-1343.